

Dark Matter Search in Space: Combined Analysis of Cosmic Ray Antiproton-to-Proton Flux Ratio and Positron Flux Measured by AMS-02

Jie Feng and Hong-Hao Zhang*

School of Physics, Sun Yat-Sen University, Guangzhou 510275, China

Dark matter search in space has been carried out for many years. Measurements of cosmic ray photons, charged antiparticles and neutrinos are useful tools for dark matter indirect search. The antiparticle energy spectra of cosmic rays have several exciting features such as the unexpected positron excess at $E \sim 10 - 500$ GeV and the remarkably flattening antiproton/proton at $E \sim 60 - 450$ GeV precisely measured by the AMS-02 experiment, which can not be explained simultaneously by secondary production in interstellar medium. In this work, we report a combined analysis of cosmic ray antiproton and positron spectra arising from dark matter on the top of a secondary production in a spatial-dependent propagation model. We discuss the systematics from antiproton production cross section using the two latest Monte Carlo generators, *i.e.* EPOS LHC and QGSJET-II-04m, respectively. We compare their results. In the case of EPOS LHC, we find that the dark matter pair annihilating into τ leptons channel with 100% branching ratio is the only possible one channel scenario to explain data. On the other hand, there is not a single possible channel in the case of QGSJET-II-04m. We also propose possible two-channel scenarios based on these two Monte Carlo generators.

I. INTRODUCTION

After nearly one century of physics investigation, the search for dark matter is still ongoing. This search is carried out in three complementary ways: dark matter production in colliders, direct detection with underground instruments and indirect detection in cosmic rays (CRs). Dark matter annihilation or decay may produce elementary particles, including neutral particles (photons (γ) and neutrinos) and charged ones (positrons (e^+) and antiprotons (\bar{p})). An impressive amount of dark matter information is being achieved by γ -ray data coming from spacebased or groundbased telescopes such as Fermi's Large Area Telescope (Fermi-LAT) [1, 2] or High Energy Stereoscopic System (H.E.S.S.) [3]. Besides, valuable pieces of dark matter information from neutrinos are being collected by IceCube [4]. At the same time, an increase in the accuracy of charged elementary CR particles spectra is driving us to a deeper understanding of the fundamental physics processes in the Galaxy. Thanks to the new generation detection experiments, such as the Payload for Antimatter Matter Exploration and Light-nuclei Astrophysics (PAMELA) or the Alpha Magnetic Spectrometer (AMS-02) in space, we are able to read dark matter information in charged particle channels. The AMS-02 collaboration has now published the precise \bar{p}/p ratio measurement between ~ 0.5 and ~ 450 GeV of kinetic energy, showing that the ratio above ~ 60 GeV experiences a remarkably flat behavior [5]. PAMELA has also published similar results but with less statistical significance [6]. Together with the recent e^+ flux data [7, 8], which shows a surprising excess above ~ 10 GeV, those results give us a hint of extra sources.

Unlike neutral particles that travel almost along

straight lines, charged particles are difficult to be traced back to their sources due to the complex magnetic turbulence in the Galaxy. To constrain secondary production contribution, one also need to study the CR B/C elemental ratio, which can be measured by PAMELA and AMS-02 in space, or by the Advanced Thin Ionization Calorimeter (ATIC-2) and the Cosmic Ray Energetics and Mass (CREAM) on balloon. Besides, systematics from solar modulation and antiparticle production cross section should also be studied [9]. Ref. [9] showed that the excess of antiprotons was not significant but that of positrons was solid given by the current understanding of systematics. Some studies were carried out to interpret the positron excess that were consistent with a smooth B/C spectrum. Unless the sources accelerating C-N-O are not the same as those accelerating helium or protons [10], it seems unavoidable to introduce extra source components such as dark matter particle annihilation [11–15], or e^\pm pair production mechanisms inside nearby pulsars [14–22]. Observations by Fermi-LAT [23] indicated that γ -rays of pulsars were produced by leptons rather than hadrons, which can basically exclude the possibility of pulsars to be high energy antiproton sources.

Numerous analyses have been performed to interpretate precise \bar{p}/p spectrum measured by AMS-02 independent of e^+ with dark matter scenarios [24–27]. There are some also some combined analysis of PAMELA \bar{p} , which has larger uncertainties, and AMS-02 e^+ [28]. In this paper, we perform a combined analysis of \bar{p}/p and e^+ in dark matter scenarios. We can reduce some uncertainty from normalization by analyzing \bar{p}/p instead of \bar{p} spectrum because p are \bar{p} progenitors. For a similar reason, we avoid injection uncertainties of e^- by analyzing e^+ instead of $e^+/(e^++e^-)$. Our basic idea is that the cross section and the mass of dark matter annihilation estimated from e^+ data should be consistent with that from \bar{p} data. Besides, we notice that antiproton production cross section introduces major systematic uncertainties

arXiv:1701.02263v3 [hep-ph] 14 Jan 2018

* zhh98@mail.sysu.edu.cn

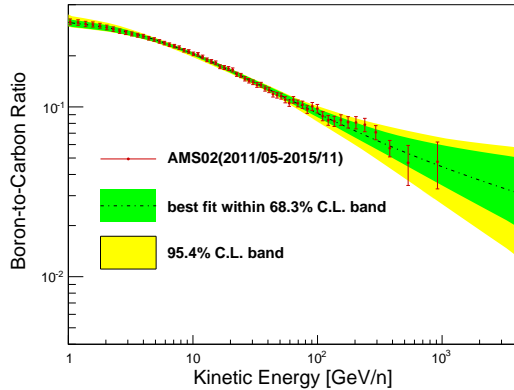


FIG. 1: Best fit model calculation and uncertainty band for the B/C ratio in comparison with AMS-02 data [30].

in \bar{p}/p spectrum [9, 29]. Following the implementation of the cross section from MC generators in [9], we present our study with EPOS LHC and QGSJET-II-04m, which were tuned against the latest LHC experimental data and reproduce the \bar{p} production well [9, 26]. We quantify the agreement between model prediction and data with “p-value” method. We find that $\chi\chi \rightarrow \tau^+\tau^-$ is the only possible channel with 100% branching ratio based on the antiproton background calculated by EPOS LHC, while no channel is possible for QGSJET-II-04m. We also study the scenarios that dark matter decays into two channels, which gives a larger p-value compared to the one from channel scenarios. Comparisons with the analysis of γ -ray observation are also shown.

This paper is organized as follows. In Sec. II, we present our calculations. In Sec. II A, we review briefly the \bar{p} and e^+ from astro-physical sources as the background of our analysis. In Sec. II B, we introduce \bar{p} and e^+ flux produced at dark matter annihilation. In Sec. II C, it is presented our definition of a good fit. In Sec. II D, our consideration of solar modulation uncertainties is shown. In Sec. III, we show our results and discussion including one annihilation channel in Sec. III A and two annihilation channels in Sec. III B. Finally, the conclusion is drawn in Sec. IV.

II. CALCULATIONS

A. Astro-physical background

In convectional CR propagation models, antiparticles are only produced in collisions of high-energy nuclei with interstellar medium (ISM). The fluxes of their progenitor nuclei and CR propagation process together determine the spectra of antiparticles. The Galactic disk is surrounded by a halo with half-thickness L . For each CR species, its propagation can be described by a two-

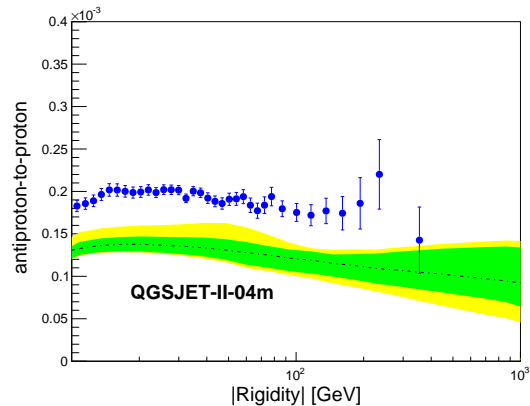
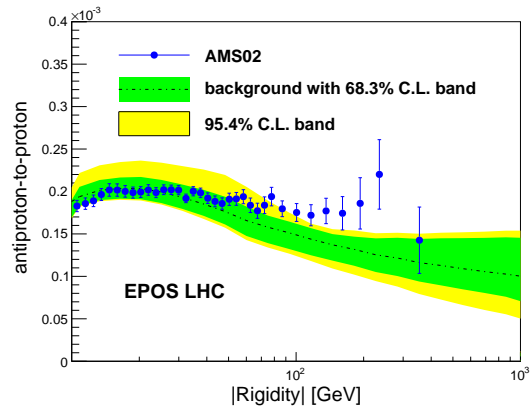


FIG. 2: Model prediction using the best fit parameters and uncertainty band for the antiproton/proton ratio. TOP: EPOS LHC hadronic model prediction. BOTTOM: QGSJET-II-04m hadronic model prediction. AMS-02 data [5] is also shown for comparison.

dimensional transport equation:

$$\frac{\partial\psi}{\partial t} = Q + \vec{\nabla} \cdot (D\vec{\nabla}\psi) - \psi\Gamma + \frac{\partial}{\partial E}(\dot{E}\psi), \quad (1)$$

where $\psi = \psi(E, r, z)$ is the number density as a function of energy and space coordinates, $\Gamma = \beta cn\sigma$ is the destruction rate in ISM, with density n , at velocity βc and cross section σ . The source term Q includes a primary term, Q_{pri} , and a secondary production term $Q_{\text{sec}} = \sum_j \Gamma_j^{\text{SP}} \psi_j$, from interaction of heavier j -type nuclei with rate Γ_j^{SP} . The term $\dot{E} = -\frac{dE}{dt}$ describes ionization and Coulomb losses, as well as radiative cooling of CR leptons. The diffusion coefficient is taken as $D(p, z) = \beta D_0 (R/R_0)^{\delta(z)}$, where D_0 shows its normalization, $R \equiv pc/Ze$ is defined as the magnetic rigidity and R_0 is its normalization rigidity. $\delta(z)$ expresses the scaling index.

Recent studies were done to get a set of injection and propagation parameters which could simultaneously reproduce a large set of nuclear data including proton and helium fluxes, the B/C elemental ratio, and the $^{10}\text{Be}/^9\text{Be}$ isotopic ratio [9, 14, 31, 32]. To assess astro-physical background of antiparticles, we adopt a spatial-

dependent model of CR diffusion [33, 34], which can explain the high-energy departures from the standard universal power-law expectations in \mathbf{p} and \mathbf{He} spectra observed by PAMELA [35] and confirmed by AMS-02 [36, 37] while the convectional models failed to do so [38]. In this scenario, the scaling index $\delta(z) = \delta_0$ in the region of $|z| < \xi L$ (inner halo) and $\delta(z) = \delta_0 + \Delta$ when $|z| \geq \xi L$ (outer halo). The normalization is D_0 for the inner halo and χD_0 for the outer. There is a connecting function of the type $F(z) = (z/L)^n$ to ensure a smooth transition of the parameters χ and Δ across the two zones [39]. The injection spectral indices of all the nuclei whose $z > 1$ all equal to ν , while that of proton is $\nu + \Delta\nu$. Based on the method presented in Ref. [9], we update our analysis on the parameters with the latest AMS-02 B/C ratio [30]. The best fit parameters are $L = 6.70kpc$, $D_0 = 2.18 \times 10^{28}cm^2/s$, $\delta_0 = 0.19$, $\Delta = 0.56$, $\xi = 0.22$, $\chi = 0.30$, $\delta\nu = 0.096$ and $\nu = 2.29$. In Fig. 1 the B/C ratio calculations are shown in comparisons with the data. We use DRAGON package [40], which is based on GALPROP package [41], to solve the transport equation.

Antiproton production cross section systematic is one of the main uncertainties of the astro-physical background. As has been studied in [9, 42], two of the most advanced Monte Carlo (MC) generators EPOS LHC [43] and QGSJET-II-04m [42] can reproduce the recent ground experiments well. However, due to the scarcity of the anti-neutron production data, we have no way to test anti-neutron production cross sections. EPOS LHC predicts the anti-neutron/anti-proton ratio varies between 1.2 and 2.0, while QGSJET-II-04m shows it is close to 1 except near the production threshold. As is shown in Fig. 2, both model predictions with the latest AMS-02 B/C data [30] on the antiproton-to-proton ratio are well above the experimental data measured by the same instrument [5]. We believe the truth should be somewhere between these two models, so we test the dark matter scenarios with the backgrounds predicted by them individually. Positron production cross section is taken from a recent parameterization [44]. As you can find latter in Sec. III, positron production cross section is not a dominating component of the total uncertainties, since the excess of e^+ from the background is significant. So we do not discuss other e^+ cross section in this paper.

Pulsars are also important sources which produce secondary positrons. Previous studies showed that it is better to explain positron spectrum with pulsar models rather than with dark matter models [15]. This is due to the fact that the profile of pulsar model usually has more degree of freedom than that of dark matter model. For example, it is unavoidable to introduce at least three parameters in the pulsar fit, *i.e.*, the cutoff energy, the injection spectral index and the normalization [22]. In dark matter scenarios, however, there are only two free parameters: the mass of the dark matter m_χ and the normalization (*i.e.* thermally averaged annihilation cross section $\langle\sigma v\rangle$ in the case of annihilation, where σ is the

annihilation cross section and v is the velocity, or τ which is the lifetime in the case of decay [24]). The γ -ray spectrum of a single pulsar is preferred to be explained by a leptonic model rather than hadronic one [23]. The spectral index of γ -ray produced from pion-decay emission [45] of hadronic interactions should be harder than that through the Inverse-Compton scattering by leptons a pulsar. Observation of RX J1713.7-3946 supports the latter one. One might easily explain the CR antiproton spectrum by dark matter and the positron by pulsar. In this way, there will be five free parameters so everything can be explained. However, this is not what we are going to do in this paper. Since the parameters of pulsars are not easy to be constrained, we do not consider contribution of them into the astro-physical background.

B. The fluxes of anti-matter from dark matter annihilation

The CR anti-particle fluxes produced by dark matter have been studied and collected in A Poor Particle Physicist Cookbook for Dark Matter Indirect Detection (PPPC) [46]. The authors calculated the results with PYTHIA and HERWIG Monte Carlos so they had a feeling of the uncertainties. Historically, leptons and vector bosons were treated as unpolarized. And parton showers were assumed not to emit W 's and Z 's. Under these assumptions, \bar{p} will not be produced in leptonic channels. However, as is pointed out by [47], polarizations and electroweak corrections should be considered, which will modify e^\pm spectra at low energies $E \ll m_\chi$ and produce \bar{p} in leptonic channels due to W/Z radiation.

We consider dark matter annihilation into the following primary channels: e^+e^- , muons ($\mu^+\mu^-$), taus ($\tau^+\tau^-$), light quarks ($q\bar{q}$), bottom quarks ($b\bar{b}$) and W bosons ($W\bar{W}$) in order to compare this study with the γ -ray observations [2]. As you can see latter in this paper, $q\bar{q}$, $b\bar{b}$ and $W\bar{W}$ predict too many \bar{p} but not enough e^+ . In order to improve the model, we also study the $VV \rightarrow 4e$, $VV \rightarrow 4\mu$ and $VV \rightarrow 4\tau$, where the annihilation first goes into a new light boson V that will later decay into a pair of leptons proposed by [48, 49]. Previous study by Ref.[50] showed that those channels can also reproduce e^+ . These so-called “4-body” channels will not produce \bar{p} . A recent study proposed a “3-body” channel where dark matter decays into a stable neutral particle and a pair of super symmetry fermions [28], which is also interesting but more complex. Another recent work proposed a new “4-body” channel that dark matter annihilate into light mediators that later decays into $2q\bar{q}$ [27]. We do not discuss this case since it produces mostly \bar{p} in its final state while we prefer more e^+ in this study.

We adopt the Navarro, Frenk and White (NFW) [51] profile to describe the galactic distribution of dark matter

in the Milky Way, which reads:

$$\rho_{\text{NFW}}(r) = \rho_s \frac{r_s}{r} \left(1 + \frac{r}{r_s}\right)^{-2}, \quad (2)$$

where $\rho_s = 0.184 \text{ GeV}/\text{cm}^3$ and $r_s = 24.42 \text{ kpc}$ are typical scale density and radius [46]. These values are obtained by setting the density to be $\rho_\odot = 0.3 \text{ GeV}/\text{cm}^3$ at the Sun position $r_\odot = 8.33 \text{ kpc}$.

After getting the fluxes of antiparticles produced by dark matter with NFW distribution, we take it as the source term in the transport equation eq. (1). The differential fluxes of antimatter at production are $Q_{\text{DM}}(E) \propto (\rho/m_\chi)^2$ in the case of annihilation and $Q_{\text{DM}}(E) \propto (\rho/m_\chi)$ in the case of decay [46]. Since the fluxes have the same energy dependence for the two cases and the energy spectra at the position of the earth would be similar, we discuss dark matter annihilation here as an example.

C. Formalism of the statistical test method

We adopt a frequentist statistical test in this work. Generally speaking, for discovering dark matter, we define the null hypothesis, H_0 , as the astrophysical background, which is to be tested against the alternative H_1 that includes both astrophysical background and dark matter signal. For setting dark matter limits, we define H_0 as the astrophysical background plus dark matter signal to be tested against the background-only hypothesis, H_1 . This work is in the former case. To quantify the agreement between data and the predictions of H , we compute the probability, the widely used ‘‘p-value’’ [52],

$$p_\theta = \int_{t_{\theta, \text{obs}}}^{\infty} f(t_\theta|\theta) dt_\theta, \quad (3)$$

where t_θ is the χ^2 for a given signal strength θ . $t_{\theta, \text{obs}}$ is the observed one. $f(t_\theta|\theta) = \frac{t_\theta^{r/2-1}}{\Gamma(\frac{r}{2})2^{r/2}} e^{-t_\theta/2}$ is the distribution of t_θ for the number of degree of freedom r , where $\Gamma(x)$ is a gamma function.

D. Solar modulation uncertainties

Force field approximation is used to describe solar modulation. However, this approximation fails to describe charge-sign-dependent solar modulation [53, 54], which is recently observed by PAMELA [55] and can be quantitatively studied with high statistic AMS data. In order to take solar modulation uncertainties into account, the χ^2 can be written as a function of $\langle\sigma v\rangle$ and the dark matter mass m_χ ,

$$\chi^2(m_\chi, \langle\sigma v\rangle, \boldsymbol{\theta}_{\text{bkg}}, \phi) = \sum_{k=1}^{N_D} \left(\frac{y_k^{\text{exp}} - y_k^{\text{th}}(m_\chi, \langle\sigma v\rangle, \boldsymbol{\theta}_{\text{bkg}}, \phi)}{\sigma_k} \right)^2 \quad (4)$$

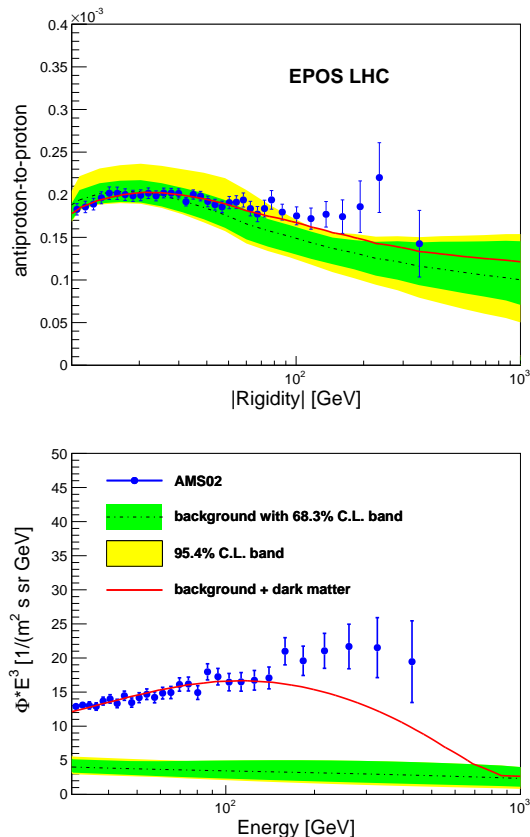


FIG. 3: Combined fit of \bar{p}/p (TOP) and e^+ (BOTTOM) for the 1-channel scenario with EPOS LHC: $\chi\chi \rightarrow \tau^+\tau^-$.

where $\sigma_k = \sqrt{\sigma_{k,0}^2 + \sigma_{k,\phi}^2}$ is the total uncertainty of the data point k with considering the model uncertainty ($\sigma_{k,\phi}$) introduced by varying the solar modulation potential ϕ from -300MV to $+700\text{MV}$. The prior of background parameters $\boldsymbol{\theta}_{\text{bkg}}$ is obtained via the fitting to the B/C [30], $^{10}\text{Be}/^9\text{Be}$ [56–61], proton [36], helium [37, 62] and carbon data [63, 64]. This quantity describes the consistency of model parameters ($m_\chi, \langle\sigma v\rangle, \boldsymbol{\theta}_{\text{bkg}}, \phi$) and experimental data (y^{exp}) with corresponding uncertainties ($\sigma_{k,0}$).

In this way, the model is more sensitive to high energy CR data rather than low energy ones. This method allows us to make use of the low energy data without introducing bias from solar modulation models.

III. RESULTS AND DISCUSSION

A. dark matter annihilation into one channel

We investigate the possibility to explain \bar{p} and e^+ by one annihilation channel with 100% branching ratio. We study \bar{p}/p spectrum instead of \bar{p} flux, since the uncertainties of \bar{p} and those of p are cancelled. To

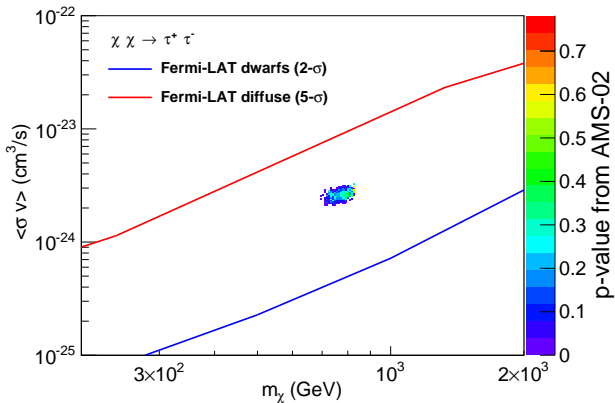


FIG. 4: AMS-02 estimation of dark matter mass m_χ for $\tau^+\tau^-$ channel with EPOS LHC, comparing with constraints from Fermi-LAT diffuse measurements [1] in red and 6-year Dwarf Spheroidal Galaxies observation [2] in blue.

avoid the uncertainties of the e^- injection spectra, we study e^+ flux. To avoid solar modulation uncertainties, we use positron flux data above 30 GeV, antiproton-to-proton flux ratio above 10 GeV, and primary fluxes above 10 GeV. We found that only $\chi\chi \rightarrow \tau^+\tau^-$ channel gives us a p-value greater than 10^{-5} , with a normalized chisquare $\chi^2/n.d.f. = 161.82/207$ and $p_{m_\chi} = 0.9918$. We get the best fit values: $m_\chi = 783 \pm 56$ GeV and $\langle\sigma v\rangle = 261.20 \pm 23.93 \times 10^{-26} \text{ cm}^3/\text{s}$. Other channels are impossible. To give a feeling of the goodness of the fit, we plot the calculated \bar{p}/p and e^+ spectra together with the AMS-02 data in Fig. 3. On the other hand, however, there is no channel that gives us a large p-value with QGSJET-II-04m.

In Fig. 4, it is shown that this scenario survives from the constraints of Fermi-LAT diffuse measurements [1] but has been excluded by γ -ray observations from Milky Way Dwarf Spheroidal Galaxies under the s-wave-dominated dark matter assumption [2]. However, there is still a possibility to accept this scenario if p-wave annihilation is not negligible, according to a recent study [65].

From this exercise, it is shown that most of the single channel scenarios can not simultaneously explain \bar{p} and e^+ . With respect to the astro-physical background, the excess of e^+ is a solid evidence of extra e^+ source, while that of \bar{p} is marginal. This requires a large $\langle\sigma v\rangle$ to explain e^+ data, while a small $\langle\sigma v\rangle$ to produce \bar{p} . For quark (*e.g.* $q\bar{q}$ and $b\bar{b}$) or boson channels (*e.g.* $W\bar{W}$), it predicts not enough e^+ and too much \bar{p} . For leptonic channels (*i.e.* e^+e^- , $\mu^+\mu^-$ and $\tau^+\tau^-$), it predicts enough e^+ but the e^+ profile of dark matter signal does not match data quite well. Thus, we introduce one more channel to get more e^+ in Sec. III B to improve the fit.

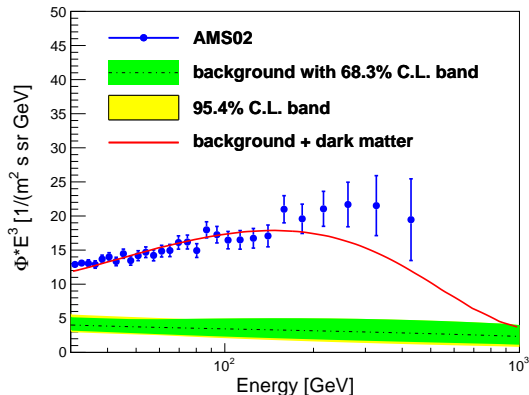
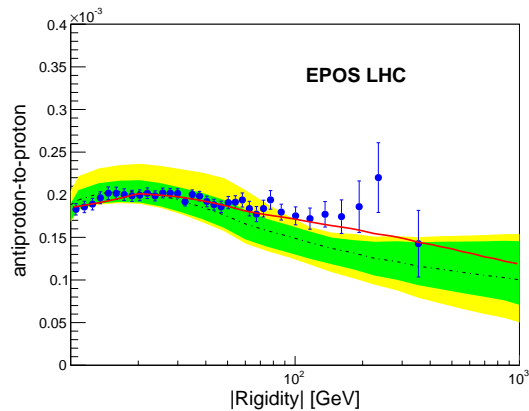


FIG. 5: Combined fit of \bar{p}/p (TOP) and e^+ (BOTTOM) for the 2-channel scenario with EPOS LHC: $\chi\chi \rightarrow W\bar{W}$ and $\chi\chi \rightarrow VV \rightarrow 2\tau^+\tau^-$.

B. dark matter annihilation into two channels

Now we come to the possibility that dark matter annihilates into two channels. In Sec. III A, it is shown that more e^+ in the annihilation will improve the fit. In addition to the 6 channels in Sec. III A, those “4-body” lepton channels have been studied as the second channels, which are pure lepton channels and do not produce any \bar{p} . In this kind of scenarios, we will have more e^+ while keeping almost the same amount of \bar{p} .

Seven scenarios with a best fit p-value greater than 10^{-7} for EPOS LHC as the antiproton production model are listed in Table. I. The number of degree of freedom is 208. CH_i stands for the i th channel. BR_i is short for the branching ratio of the i th channel. Compared with the one channel scenarios, these two channel scenarios can improve the quality of the fit a lot. In Table. I, it is shown that $\chi\chi \rightarrow VV \rightarrow 2\tau^+\tau^-$ is the dominating channel in three scenarios with the largest p-values. For QGSJET-II-04m, no scenario gives a p-value greater than 10^{-7} . The best scenario gives a $\chi^2/n.d.f. = 349.11/208$ and a p-value = 3.1×10^{-9} with the parameters: $m_\chi = 545 \text{ GeV}$, $\langle\sigma v\rangle \times BR_1 = 3.45 \times 10^{-26} \text{ cm}^3/\text{s}$ for $\chi\chi \rightarrow q\bar{q}$ and $\langle\sigma v\rangle \times BR_2 = 74.47 \times 10^{-26} \text{ cm}^3/\text{s}$ for $\chi\chi \rightarrow VV \rightarrow$

| CH_1 | CH_2 | m_χ (GeV) | $\langle\sigma v\rangle \times BR_1$ ($10^{-26} \text{cm}^3/\text{s}$) | $\langle\sigma v\rangle \times BR_2$ ($10^{-26} \text{cm}^3/\text{s}$) | χ^2 | p-value |
|----------------|--------------------------------|-------------------|---|---|----------|---------|
| $\tau^+\tau^-$ | $VV \rightarrow 2\tau^+\tau^-$ | 1320 ± 14 | 225.29 ± 7.39 | 244.48 ± 9.38 | 164.42 | 0.9885 |
| $q\bar{q}$ | $VV \rightarrow 2\mu^+\mu^-$ | 654 ± 12 | 0.96 ± 0.14 | 89.85 ± 5.7 | 174.85 | 0.9593 |
| $q\bar{q}$ | $VV \rightarrow 2\tau^+\tau^-$ | 1800 ± 23 | 3.97 ± 0.08 | 588.71 ± 12.53 | 162.43 | 0.9916 |
| $b\bar{b}$ | $VV \rightarrow 2\mu^+\mu^-$ | 601 ± 12 | 1.00 ± 0.16 | 81.89 ± 5.46 | 185.60 | 0.8659 |
| $b\bar{b}$ | $VV \rightarrow 2\tau^+\tau^-$ | 1679 ± 34 | 4.38 ± 0.16 | 598.98 ± 15.94 | 149.29 | 0.9992 |
| $W\bar{W}$ | $VV \rightarrow 2\mu^+\mu^-$ | 624 ± 11 | 1.45 ± 0.16 | 87.59 ± 6.59 | 180.12 | 0.9192 |
| $W\bar{W}$ | $VV \rightarrow 2\tau^+\tau^-$ | 1689 ± 23 | 5.34 ± 0.10 | 594.68 ± 17.96 | 143.65 | 0.9998 |

TABLE I: m_χ s, $\langle\sigma v\rangle$ s, χ^2 s and p-values given by the “Good” fits in two-channel scenarios with EPOS LHC. The number of degree of freedom is 208.

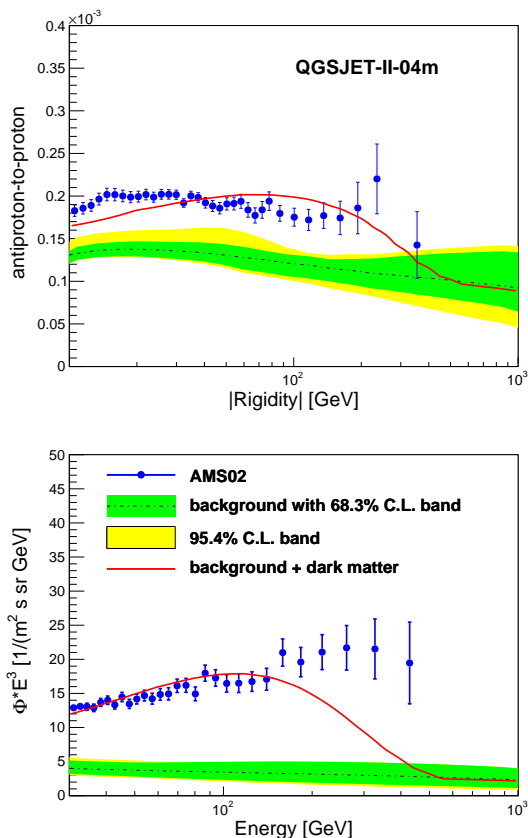


FIG. 6: Combined fit of \bar{p}/p (TOP) and e^+ (BOTTOM) for the 2-channel scenario with QGSJET-II-04m: $\chi\chi \rightarrow q\bar{q}$ and $\chi\chi \rightarrow VV \rightarrow 2\mu^+\mu^-$.

$2\mu^+\mu^-$.

We draw the \bar{p}/p and e^+ plots of dark matter annihilation into $W\bar{W}$ and $VV \rightarrow 2\tau^+\tau^-$ channel as the “best” fit example for EPOS LHC in Fig. 5. This scenario shows the mass of dark matter is 1689 ± 23 GeV and its $\langle\sigma v\rangle = 600.02 \pm 21.32 \times 10^{-26} \text{cm}^3/\text{s}$ with a branching ratio of $0.890 \pm 0.017\%$ for $\chi\chi \rightarrow W\bar{W}$ and that of $99.11 \pm 0.03\%$ for $\chi\chi \rightarrow VV \rightarrow 2\tau^+\tau^-$. In Fig. 6, it is shown the \bar{p}/p and e^+ plots of dark matter annihilation into $q\bar{q}$

and $VV \rightarrow 2\mu^+\mu^-$ channel for QGSJET-II-04m. This fit gives a low p-value, which is 3.1×10^{-9} . We obtain that the mass of dark matter is 545 ± 20 GeV and its $\langle\sigma v\rangle = 77.92 \pm 4.08 \times 10^{-26} \text{cm}^3/\text{s}$ with a branching ratio of $4.42 \pm 0.17\%$ for $\chi\chi \rightarrow q\bar{q}$ and that of $95.57 \pm 0.16\%$ for $\chi\chi \rightarrow VV \rightarrow 2\mu^+\mu^-$.

These two plots show that the two antiproton production models do not give consistent results for all the scenarios. As is discussed in Sec. II A, the difference of anti-neutron production in these two MC generators is the source of the systematics of the antiproton astrophysical background. Some recent works parameterized the antiproton production cross sections with the latest ground experimental data [29, 66], which is also a good way to obtain this cross section. For antineutron production, however, they assumed an energy independent scale factor $\kappa \equiv \text{antineutron}/\text{antiproton}$ to be a constant according to isospin symmetry, based on a preliminary experimental result published in a conference proceeding [67]. One should notice that this energy independent assumption of κ is not precise enough to describe antineutron production. When the antiproton energy is close to the production threshold, κ should be maximum in any model. κ goes down when the antiproton energy moves away from the threshold [9]. An energy dependent κ , however, changes the shape of the \bar{p} flux. More cross section measurement data from accelerators will help to reduce this kind of systematic errors.

Since both of these two generators predict a \bar{p}/p astrophysical background going down with energy above 60 GeV where AMS-02 data shows no energy dependence, a hint of an extra \bar{p} source like dark matter is seen in the top plots of Fig. 5 and Fig. 6. The dark matter signal makes the \bar{p}/p spectrum harder and closer to observed data. However, compared to the uncertainties of the astro-physical background, the signal of dark matter is not very significant. On the other hand, e^+ flux measured by AMS-02 is significantly higher than astrophysical background. The dark matter profile can produce a “cut-off” like spectrum as is measured by AMS-02. The “best” fit results can match measurement up to a few hundred GeV.

IV. CONCLUSIONS

An increase in the accuracy of the CR antiparticle spectra measurements is driving us closer to the answer of dark matter. Together with CR γ -ray [1–3] and neutrino [4] spectra, \bar{p} and e^+ spectra help us study astrophysical properties of the potential dark matter with $m_\chi \sim 10^0 - 10^5$ GeV.

We summarize everything here. We present our study on dark matter search from CR \bar{p} and e^+ data above 30 GeV. For the first time, we simultaneously interpretate \bar{p} and e^+ spectra in the framework of AMS-02 with dark matter scenarios. We find that $\chi\chi \rightarrow \tau^+\tau^-$ channel with 100% branching ratio is the best one channel scenario to reproduce CR \bar{p}/p and e^+ flux measurement, with $m_\chi = 783 \pm 56$ GeV and $\langle\sigma v\rangle = 261.20 \pm 23.93 \times 10^{-26} \text{cm}^3/\text{s}$, in the case of EPOS LHC. For the antiproton background using the same MC generator, we also propose a two channel scenario: $m_\chi = 1689 \pm 23$ GeV and $\langle\sigma v\rangle = 600.02 \pm 21.32 \times 10^{-26} \text{cm}^3/\text{s}$. The dominating channel is $\chi\chi \rightarrow VV \rightarrow 2\tau^+\tau^-$ with a branching ratio of $99.11 \pm 0.03\%$, while the second channel is $\chi\chi \rightarrow W\bar{W}$ with a branching ratio of $0.890 \pm 0.017\%$. In the case of QGSJET-II-04m, no scenario gives a good fit. These scenarios predict \bar{p}/p spectra harder than those in the background only scenario. They also predict a e^+ spectrum with a cut off between 100 and 2000 GeV, which is also observed by AMS-02, even though the shape does not completely match data.

Comparing to the pulsar scenarios [22], we find that the $\chi^2/n.d.f.s$ in dark matter fits are higher. This is due to the fact that pulsar models usually have more degrees of freedom. For example, the injection spectral index of a pulsar is a free parameter, which will adjust the pulsar profile to match e^+ data. On contrast, the spectral index of e^+ flux produced by dark matter is fixed by theoretical

models. It is necessary to have some models to constrain the spectral index of a pulsar or to link it with the corresponding γ -ray spectrum. Moreover, if one tries to perform a combined fit on \bar{p}/p and e^+ spectra with quark channel dark matter and pulsar model, he has 2+3=5 free parameters and will obtain a good fit. Here we have only 3 free parameters for two channel dark matter scenario. We also investigate the impact of the antiproton background caused by cross sections. Two of the most advanced MC generators, EPOS LHC and QGSJET-II-04m, do not give consistent results. This systematics is due to the lack of knowledge of anti-neutron production, which could be supplemented with new data of future underground experiments.

To perform a dark matter search below 30 GeV, we have to reduce the uncertainties from solar modulation, as is pointed out by a recent study [9]. Recent time dependent e^+/e^- measurements by PAMELA [55] confirmed charge-sign-dependent solar modulation models [53, 54]. The convectional force field approximation [68] is not precise enough for us. AMS-02 will publish its much more precise time-dependent e^+ , e^- , \bar{p} and p fluxes in the near future, which will make it possible for us to reconstruct the fluxes out of the heliosphere. We look forward to searching for dark matter below 30 GeV at that time.

ACKNOWLEDGMENTS

We thank Qiang Yuan and Zhao-Huan Yu for helpful discussions. This work is supported by the National Natural Science Foundation of China (NSFC) under Grant Nos. 11375277, 11410301005, 11647606, and 11005163, the Fundamental Research Funds for the Central Universities, the Natural Science Foundation of Guangdong Province under Grant No. 2016A030313313, and the Sun Yat-Sen University Science Foundation.

-
- [1] M. Ackermann et al. (Fermi-LAT), *Astrophys. J.* **761**, 91 (2012), [arXiv:1205.6474 \[astro-ph.CO\]](#).
 - [2] M. Ackermann et al. (Fermi-LAT), *Phys. Rev. Lett.* **115**, 231301 (2015), [arXiv:1503.02641 \[astro-ph.HE\]](#).
 - [3] H. Abdallah et al. (HESS), *Phys. Rev. Lett.* **117**, 111301 (2016), [arXiv:1607.08142 \[astro-ph.HE\]](#).
 - [4] M. G. Aartsen et al. (IceCube), *Eur. Phys. J.* **C76**, 531 (2016), [arXiv:1606.00209 \[astro-ph.HE\]](#).
 - [5] M. Aguilar et al. (AMS), *Phys. Rev. Lett.* **117**, 091103 (2016).
 - [6] O. Adriani et al., *JETP Lett.* **96**, 621 (2013), [*Pisma Zh. Eksp. Teor. Fiz.*96,693(2012)].
 - [7] O. Adriani et al. (PAMELA), *Nature* **458**, 607 (2009), [arXiv:0810.4995 \[astro-ph\]](#).
 - [8] M. Aguilar et al. (AMS), *Phys.Rev.Lett.* **113**, 121102 (2014).
 - [9] J. Feng, N. Tomassetti, and A. Oliva, *Phys. Rev.* **D94**, 123007 (2016), [arXiv:1610.06182 \[astro-ph.HE\]](#).
 - [10] N. Tomassetti and J. Feng, *Astrophys. J.* **835**, L26 (2017), [arXiv:1612.05651 \[astro-ph.HE\]](#).
 - [11] M. Cirelli and A. Strumia, ArXiv e-prints (2008), [arXiv:0808.3867](#).
 - [12] M. Cirelli, M. Kadastik, M. Raidal, and A. Strumia, *Nucl.Phys.* **B813**, 1 (2009), [arXiv:0809.2409 \[hep-ph\]](#).
 - [13] Q. Yuan, X.-J. Bi, G.-M. Chen, Y.-Q. Guo, S.-J. Lin, et al., *Astropart.Phys.* **60**, 1 (2015), [arXiv:1304.1482 \[astro-ph.HE\]](#).
 - [14] S.-J. Lin, Q. Yuan, and X.-J. Bi, *Physical Review D* **91**, 063508 (2015), [arXiv:1409.6248 \[astro-ph.HE\]](#).
 - [15] M. Boudaud, S. Aupetit, S. Caroff, A. Putze, G. Belanger, Y. Genolini, C. Goy, V. Poireau, V. Poulin, S. Rosier, P. Salati, L. Tao, and M. Vecchi, *Astron.Astrophys.* **575**, A67 (2015), [arXiv:1410.3799 \[astro-ph.HE\]](#).
 - [16] D. Hooper, P. Blasi, and P. D. Serpico, *JCAP* **0901**, 025 (2009), [arXiv:0810.1527 \[astro-ph\]](#).

- [17] S. Profumo, *Central Eur.J.Phys.* **10**, 1 (2011), [arXiv:0812.4457 \[astro-ph\]](#).
- [18] T. Delahaye, J. Lavalle, R. Lineros, F. Donato, and N. Fornengo, *Astron.Astrophys.* **524**, A51 (2010), [arXiv:1002.1910 \[astro-ph.HE\]](#).
- [19] T. Linden and S. Profumo, *Astrophys.J.* **772**, 18 (2013), [arXiv:1304.1791 \[astro-ph.HE\]](#).
- [20] P.-F. Yin, Z.-H. Yu, Q. Yuan, and X.-J. Bi, *Phys.Rev.* **D88**, 023001 (2013), [arXiv:1304.4128 \[astro-ph.HE\]](#).
- [21] T. Delahaye, K. Kotera, and J. Silk, *Astrophys.J.* **794**, 168 (2014), [arXiv:1404.7546 \[astro-ph.HE\]](#).
- [22] J. Feng and H.-H. Zhang, *Eur. Phys. J.* **C76**, 229 (2016), [arXiv:1504.03312 \[hep-ph\]](#).
- [23] A. A. Abdo et al., *Astrophysical Journal* **734**, 28 (2011), [arXiv:1103.5727 \[astro-ph.HE\]](#).
- [24] G. Giesen, M. Boudaud, Y. Genolini, V. Poulin, M. Cirelli, P. Salati, and P. D. Serpico, *JCAP* **1509**, 023 (2015), [arXiv:1504.04276 \[astro-ph.HE\]](#).
- [25] S.-J. Lin, X.-J. Bi, P.-F. Yin, and Z.-H. Yu, (2015), [arXiv:1504.07230 \[hep-ph\]](#).
- [26] S.-J. Lin, X.-J. Bi, X. X, P.-F. Yin, and Z.-H. Yu, (2016), [arXiv:1612.04001 \[astro-ph.HE\]](#).
- [27] X.-J. Huang, C.-C. Wei, Y.-L. Wu, W.-H. Zhang, and Y.-F. Zhou, (2016), [arXiv:1611.01983 \[hep-ph\]](#).
- [28] H.-C. Cheng, W.-C. Huang, X. Huang, I. Low, Y.-L. S. Tsai, and Q. Yuan, (2016), [arXiv:1608.06382 \[hep-ph\]](#).
- [29] M. Di Mauro, F. Donato, N. Fornengo, R. Lineros, and A. Vittino, *JCAP* **1404**, 006 (2014), [arXiv:1402.0321 \[astro-ph.HE\]](#).
- [30] M. Aguilar et al. (AMS), *Phys. Rev. Lett.* **117**, 231102 (2016).
- [31] G. G. Johannesson et al., *Astrophys. J.* **824**, 16 (2016).
- [32] C. Evoli, D. Gaggero, and D. Grasso, *JCAP* **1512**, 039 (2015), [arXiv:1504.05175 \[astro-ph.HE\]](#).
- [33] N. Tomassetti, *Astrophys. J.* **752**, L13 (2012), [arXiv:1204.4492 \[astro-ph.HE\]](#).
- [34] N. Tomassetti, *Phys. Rev. D* **92**, 081301 (2015), [arXiv:1509.05775 \[astro-ph.HE\]](#).
- [35] O. Adriani et al. (PAMELA), *Science* **332**, 69 (2011), [arXiv:1103.4055 \[astro-ph.HE\]](#).
- [36] M. Aguilar et al. (AMS Collaboration), *Phys. Rev. Lett.* **114**, 171103 (2015).
- [37] M. Aguilar et al. (AMS), *Phys. Rev. Lett.* **115**, 211101 (2015).
- [38] C. Evoli and H. Yan, *Astrophys. J.* **782**, 36 (2014), [arXiv:1310.5732 \[astro-ph.HE\]](#).
- [39] Y.-Q. Guo, Z. Tian, and C. Jin, (2015), [arXiv:1509.08227 \[astro-ph.HE\]](#).
- [40] D. Gaggero, L. Maccione, G. Di Bernardo, C. Evoli, and D. Grasso, *Phys.Rev.Lett.* **111**, 021102 (2013), [arXiv:1304.6718 \[astro-ph.HE\]](#).
- [41] A. W. Strong, I. V. Moskalenko, and V. S. Ptuskin, *Ann.Rev.Nucl.Part.Sci.* **57**, 285 (2007), [arXiv:astro-ph/0701517 \[astro-ph\]](#).
- [42] M. Kachelriess, I. V. Moskalenko, and S. S. Ostapchenko, *Astrophys. J.* **803**, 54 (2015), [arXiv:1502.04158 \[astro-ph.HE\]](#).
- [43] T. Pierog, I. Karpenko, J. M. Katzy, E. Yatsenko, and K. Werner, *Phys. Rev. C* **92**, 034906 (2015), [arXiv:1306.0121 \[hep-ph\]](#).
- [44] T. Kamae, N. Karlsson, T. Mizuno, T. Abe, and T. Koi, *Astrophys. J.* **647**, 692 (2006), [Erratum: *Astrophys. J.* 662,779(2007)], [arXiv:astro-ph/0605581 \[astro-ph\]](#).
- [45] D. C. Ellison and A. Vladimirov, *Astrophys. J.* **673**, L47 (2008), [arXiv:0711.4389 \[astro-ph\]](#).
- [46] M. Cirelli, G. Corcella, A. Hektor, G. Hutsi, M. Kadastik, P. Panci, M. Raidal, F. Sala, and A. Strumia, *JCAP* **1103**, 051 (2011), [Erratum: *JCAP*1210,E01(2012)], [arXiv:1012.4515 \[hep-ph\]](#).
- [47] P. Ciafaloni, D. Comelli, A. Riotto, F. Sala, A. Strumia, and A. Urbano, *JCAP* **1103**, 019 (2011), [arXiv:1009.0224 \[hep-ph\]](#).
- [48] N. Arkani-Hamed, D. P. Finkbeiner, T. R. Slatyer, and N. Weiner, *Phys. Rev.* **D79**, 015014 (2009), [arXiv:0810.0713 \[hep-ph\]](#).
- [49] M. Pospelov and A. Ritz, *Phys. Lett.* **B671**, 391 (2009), [arXiv:0810.1502 \[hep-ph\]](#).
- [50] I. Cholis and D. Hooper, *Phys.Rev.* **D89**, 043013 (2014), [arXiv:1312.2952 \[astro-ph.HE\]](#).
- [51] J. F. Navarro, C. S. Frenk, and S. D. M. White, *Astrophys. J.* **462**, 563 (1996), [arXiv:astro-ph/9508025 \[astro-ph\]](#).
- [52] G. Cowan, K. Cranmer, E. Gross, and O. Vitells, *European Physical Journal C* **71**, 1554 (2011), [arXiv:1007.1727 \[physics.data-an\]](#).
- [53] L. Maccione, *Phys. Rev. Lett.* **110**, 081101 (2013), [arXiv:1211.6905 \[astro-ph.HE\]](#).
- [54] R. Kappl, *Comput. Phys. Commun.* **207**, 386 (2016), [arXiv:1511.07875 \[astro-ph.SR\]](#).
- [55] O. Adriani et al., *Phys. Rev. Lett.* **116**, 241105 (2016), [arXiv:1606.08626 \[astro-ph.HE\]](#).
- [56] F. A. Hagen, A. J. Fisher, and J. F. Ormes, *Astrophysical Journal* **212**, 262 (1977).
- [57] A. Buffington, C. D. Orth, and T. S. Mast, *Astrophysical Journal* **226**, 355 (1978).
- [58] W. R. Webber and J. Kish, *International Cosmic Ray Conference* **1**, 389 (1979).
- [59] M. Garcia-Munoz, G. M. Mason, and J. A. Simpson, *Astrophysical Journal* **217**, 859 (1977).
- [60] M. Garcia-Munoz, J. A. Simpson, and J. P. Wefel, *International Cosmic Ray Conference* **2**, 72 (1981).
- [61] M. E. Wiedenbeck and D. E. Greiner, *Astrophysical Journal* **239**, L139 (1980).
- [62] Y. S. Yoon et al., *Astrophys. J.* **728**, 122 (2011), [arXiv:1102.2575 \[astro-ph.HE\]](#).
- [63] O. Adriani, G. Barbarino, G. Bazilevskaia, R. Bellotti, M. Boezio, et al., *Astrophys.J.* **791**, 93 (2014), [arXiv:1407.1657 \[astro-ph.HE\]](#).
- [64] H. S. Ahn et al., *Astrophys. J.* **707**, 593 (2009), [arXiv:0911.1889 \[astro-ph.HE\]](#).
- [65] Y. Zhao, X.-J. Bi, H.-Y. Jia, P.-F. Yin, and F.-R. Zhu, *Phys. Rev.* **D93**, 083513 (2016), [arXiv:1601.02181 \[astro-ph.HE\]](#).
- [66] R. Kappl and M. W. Winkler, *JCAP* **1409**, 051 (2014), [arXiv:1408.0299 \[hep-ph\]](#).
- [67] H. G. Fischer, *Heavy Ion Phys.* **17**, 369 (2003).
- [68] L. J. Gleeson and W. I. Axford, *Astrophys. J.* **154**, 1011 (1968).